Available online at www.sciencedirect.com

ScienceDirect

journal homepage: www.elsevier.com/locate/he

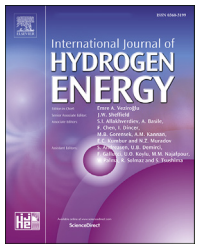

Experimental investigations of AB_5-type alloys for hydrogen separation from biological gas streams

A.N. Kazakov [a,*], I.A. Romanov [a], S.V. Mitrokhin [b], E.A. Kiseleva [a]

[a] Joint Institute for High Temperatures, Moscow, Russia
[b] Lomonosov Moscow State University, Moscow, Russia

HIGHLIGHTS

- AB_5 type alloys were studied as materials for biohydrogen purification.
- Investigated alloys have low equilibrium pressures and hydrogen capacity 1.1 %wt.
- Two alloys supposed to be used in tubular MH reactor for hydrogen separation.
- Powder bed porosity and mean particle size are defined experimentally.
- Powder bed permeabilities for alloys are calculated by Kozeny-Carman equation.

ARTICLE INFO

Article history:
Received 4 July 2019
Received in revised form
7 November 2019
Accepted 28 November 2019
Available online 23 December 2019

Keywords:
Intermetallic compound
Metal hydride
Hydrogen storage
Hydrogen separation
Biohydrogen
Bed permeability

ABSTRACT

AB_5-type intermetallic compounds are suitable materials for hydrogen separation due to their ability selectively absorb hydrogen from different gas streams, including biologically produced ones. Recent studies show that metal hydride-based purification systems can effectively extract hydrogen from biogas with high CO_2 concentration. Alloys $LaNi_{5-x}M_x$ (M = Fe, Al, Mn, Sn) are prepared and activated during several cycles of H_2 sorption/desorption and their PCT properties are measured in Sievert's type apparatus. Two compositions $LaNi_{4.4}Fe_{0.3}Al_{0.3}$ and $LaNi_{4.6}Mn_{0.2}Al_{0.2}$ are chosen for further investigations because they meet the requirements for biohydrogen separation system. After PCT measurements of 50-g samples, metal hydride powders are investigated by means of Quantochrome Nova 1200 and scanning electron microscopy to determine porosity, average particle size, specific surface area and permeability of metal hydride bed. Powder bed permeabilities are defined as 9.08×10^{-13} m^2 for $LaNi_{4.4}Fe_{0.3}Al_{0.3}$ and 6.86×10^{-13} m^2 for $LaNi_{4.6}Mn_{0.2}Al_{0.2}$ by Kozeny-Carman equation. AB_5 type $LaNi_{4.4}Fe_{0.3}Al_{0.3}$ and $LaNi_{4.6}Mn_{0.2}Al_{0.2}$ alloys show good characteristics: low equilibrium pressures 0.025–0.03 MPa and acceptable reversible hydrogen capacity 1.1 %wt. for stationary hydrogen separation system.

* *Corresponding author.*
E-mail address: h2lab@mail.ru (A.N. Kazakov).
https://doi.org/10.1016/j.ijhydene.2019.11.207

Introduction

One of the biggest challenges in the world is to meet the growing energy demands in an environmentally-benign and sustainable manner. There is an urgent need to source clean alternative and sustainable fuel to replace existing non-renewable fossil fuels. Renewable energy sources can reduce, and ultimately eliminate, greenhouse gases emissions related to fossil-fuel combustion. Unfortunately, most of renewables (wind, solar) has inherent intermittent nature and fluctuations through time [1,2].

On the other hand, biomass is a perspective renewable energy source, which is widespread throughout the world [3]. There are different pathways to produce energy from biomass both thermochemical such as gasification, reforming and partial oxidation and biological such as anaerobic digestion process or photofermentative process through hydrogen production [4,5]. Biologically produced hydrogen is called "biohydrogen". Biological processes have a specific advantage for the efficient conversion of biomass with high moisture content to pure hydrogen [6]. Anaerobic digestion so-called "dark fermentation" is a promising method to reduce different high carbon containing wastes (municipal, food, crops, etc.) and produce hydrogen. Recent researches of economic feasibility of biohydrogen technology show a high market potential [7,8]. Nevertheless, the gas mixture obtained from the fermentation process primarily containing hydrogen and other gases such as carbon dioxide is not appropriate for direct utilization. In addition, produced hydrogen in a bioreactor should be removed because its high concentration inhibits further hydrogen production and more volatile fatty acids are produced [9]. Thus, hydrogen removal and separation are significant issue for biohydrogen utilization.

The main industrial scale hydrogen separation technologies are pressure swing absorption (PSA), cryogenic distillation and metallic membranes, which have been widely applied in chemical and petrochemical industries [10,11]. Different PSA methods with elevated temperatures or MOF materials are proposed for hydrogen separation [12,13]. Combined membrane-PSA process is simulated for different biohydrogen concentrations and economic analysis is conducted [14]. Unfortunately, good results are obtained for higher pressures and temperatures, what makes PSA method energy-intensive. And as a result, PSA method might be inappropriate for small scale biohydrogen production plants. Different types of organic polymer membranes seem to be more suitable for biohydrogen separation [15–18]. Bakonyi et al. [19,20] proposed a concept of gas separation membrane bioreactor for direct hydrogen separation. However, final hydrogen concentration is around 80–85%, what is insufficient for direct use in PEM fuel cells. Maximum power generations were 9.16 W and 8.60 W for 10% and 20% CO_2 concentration, respectively. The reason for power loss was due to catalyst layer has been occupied by carbon dioxide and carbon dioxide limited hydrogen oxidation [21].

Since early 1970s intermetallic compounds are proposed as perspective materials for several practical applications: hydrogen storage [22–30], hydrogen compression [31–35], heating and cooling thermal machines [36–39], as well as hydrogen separation [40,41]. AB_5 type intermetallic compounds are implemented for hydrogen recovery from ammonia production plants [42–44]. The mobile metal hydride hydrogen separation plant, containing 1600 kg of $MlNi_{5-x}Al_x$, stored 200 Nm^3 H_2 from pretreated purge gas with hydrogen content about 50% with recovery ratio above 70% [44].

Thus, metal hydride hydrogen separation system can be a promising solution for small-scale power plant based on biohydrogen utilization. Dimanta et al. [45] presented metal hydride hydrogen accumulation from liquid phase during anaerobic fermentation. Miura et al. [46–48] presented 100Nl/h lab scale and 3 Nm^3/h bench scale systems based on metal hydrides for hydrogen extraction from reforming gas. Our research team [49] showed practical applicability of metal hydride technology for biohydrogen separation from different gas compositions. Separation of hydrogen by flow-through technique was applied in tubular metal hydride reactor with external and internal heat exchangers. Surface modification (fluorination, electroless deposition, etc.) of metal hydrides was applied to improve poisoning tolerance against CO and CO_2 [50–53]. However, metal hydrides with low equilibrium pressures are necessary for direct hydrogen separation because hydrogen partial pressure does not exceed 0.04–0.06 MPa in produced biogas [10,49,54,55].

$LaNi_5$ based alloys are chosen as hydrogen storage materials suitable for hydrogen separation due to their near-ambient PCT-properties, ease of activation without any heating, absence of protective oxide layers, possibility to regenerate H_2 capacity after interaction with H_2O or CO_2 by mild heating in hydrogen atmosphere, good cyclic stability and acceptable hydrogen storage properties for stationary applications.

Experimental procedure

We have prepared $LaNi_{5-x}M_x$ alloys with different combination of substituting elements by arc melting of pure La (99.9%), Ni (99.95%), Fe (99.99%), Al (99.9%), Mn (99.9%) and Sn (99%) several times in a water-cooled copper crucible under argon atmosphere. In each case, we added 2% to calculated weight of Sn, Al and Mn in order to compensate evaporation during the melting process. At first the furnace chamber was vacuumed to a final pressure of $4 \cdot 10^{-5}$ Pa and subsequently purged three times with argon at 41 kPa. Pure elements were joined together at a low voltage and were melt later 3 times at full power. Each melting step lasted about 1 min. After each step, alloy ingots were cooled and turned upside down. The resulting alloy ingots weighted 40–50 g each. Due to mild conditions and short time of melting steps, the weight losses of samples did not exceed 0.5% of initial metals' weight.

In order to determine structural parameters, powder samples were measured at room temperature by X-ray diffraction (XRD) using D8 Advance (Bruker) diffractometer with Cu Ka radiation. Samples for X-ray analysis were prepared by mechanical grinding to a fine powder. The step size was 0.02° and the exposition time was 1 s. The 2θ angles scanned were in the range from 20 to 90. Processing of diffraction patterns was performed using Jana2006 and Crystal Impact Match software using JCPDS PDF-2 Data Base.

At preliminary stage hydrogen sorption properties were measured by small-scale Pressure-Concentration-Temperature (PCT) measurement equipment. Experimental technique is described in more detail in Ref. [10]. PCT measurements of 50 g metal hydride samples were conducted by a Sievert's method using US150 experimental setup [56]. The purpose of US150 is a measurement of the sorption/desorption isotherms of samples mass of 10–800 g in temperature and hydrogen pressure range 243–673 K and 0–15 MPa, respectively. Activation procedure includes 10 cycles of hydrogen absorption at 5 MPa and 353 K and desorption during 4 h each cycle. After the measurements, the metal hydride reactor was fully evacuated to residual pressure 10^{-5} Pa at 373 K, cooled down, filled by inert gas to avoid ignition of the activated powder, and then opened to the air.

Activated metal hydride powders were investigated by means of scanning electron microscop Tescan VEGA with EDX Oxford Instruments INCAx-act, granulometry and liquid nitrogen gas adsorption analysis Quantochrome Nova 1200 to define powder particle size, sample porosity and bed permeability.

Results and discussion

Hydrogen sorption properties

Partial substitution of Ni by Fe, Sn, Al, Mn in different combinations are used to decrease hydrogen equilibrium pressure to meet requirements for effective biohydrogen separation. The XRD measurements of prepared alloys have shown quiet good homogeneity of the samples (Fig. 1).

Crystal structures of AB_5 alloys belong to $CaCu_5$ type. However, Sn-substituted alloys tend to be unstable. There is a peak broadening for all Sn-substituted samples. XRD pattern of $LaNi_{4.4}Fe_{0.3}Sn_{0.3}$ has splitting of main peaks of $CaCu_5$ structure. A similar behavior is obtained for $NdNi_{4.6}Sn_{0.4}$ in Ref. [57]. Phase analysis of Sn-substituted samples by Crystal Impact Match does not show existence of secondary phase other than $CaCu_5$. Sn-containing ternary AB_5 intermetallic compounds show good phase stability with Sn concentration up to $x = 0.5$ in composition $AB_{5-x}Sn_x$ [58,59]

Preliminary tests of hydrogen sorption properties are conducted to define alloy compositions suitable for direct hydrogen sorption from biohydrogen product gas. PCT curves at room temperature 295 K are shown in Fig. 2. A dotted line indicates H_2 partial pressure in biohydrogen. All samples show quite similar reversible hydrogen storage capacity in range 0.9–1.1 %wt. However, only $LaNi_{4.4}Fe_{0.3}Al_{0.3}$ and $LaNi_{4.6}Mn_{0.2}Al_{0.2}$ alloys have equilibrium hydrogen pressure under the setted hydrogen partial pressure in whole plateau region. It is important to use maximum reversible capacity for practical application to enhance overall performance of the separation system. These alloys are chosen for further investigation.

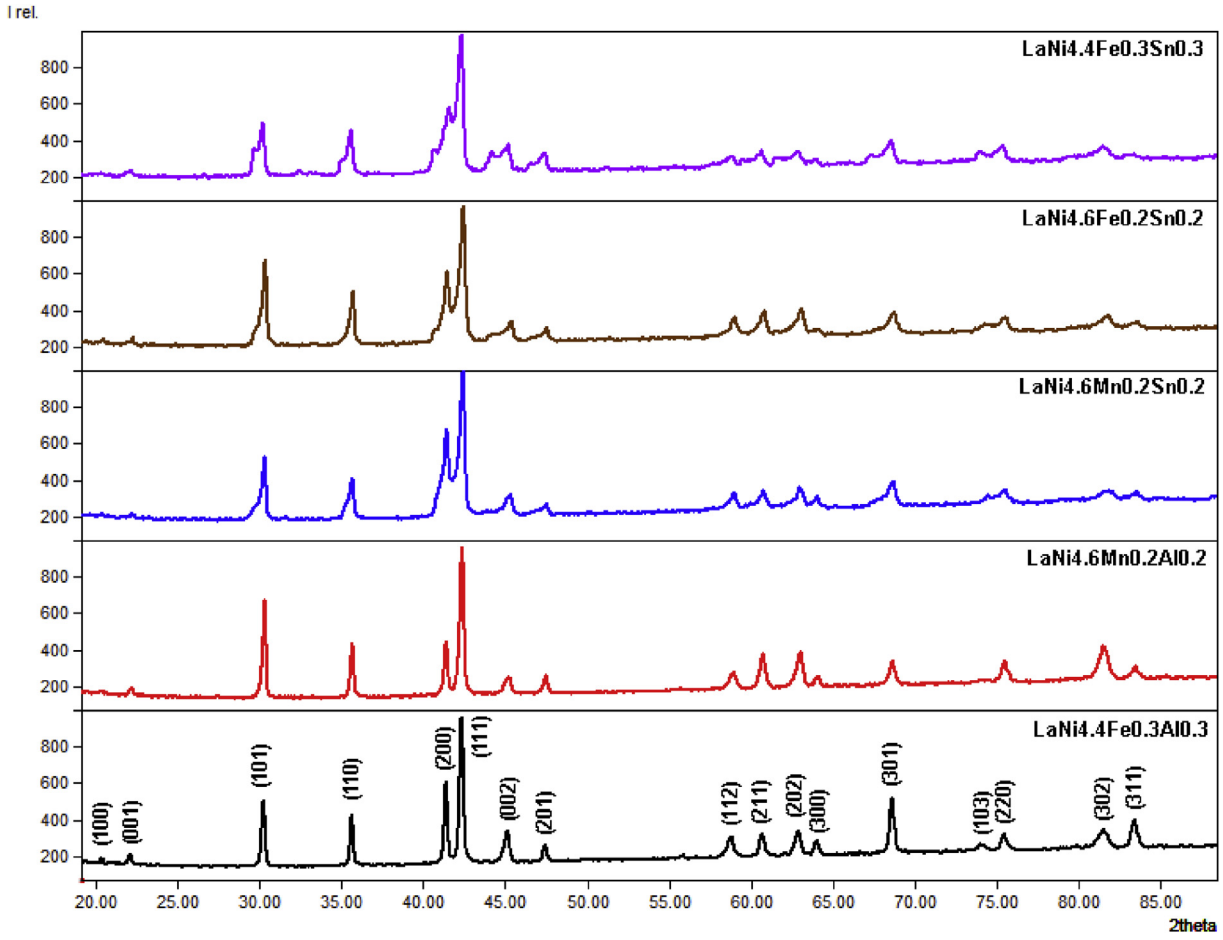

Fig. 1 – XRD of $LaNi_5$ based as cast alloys.

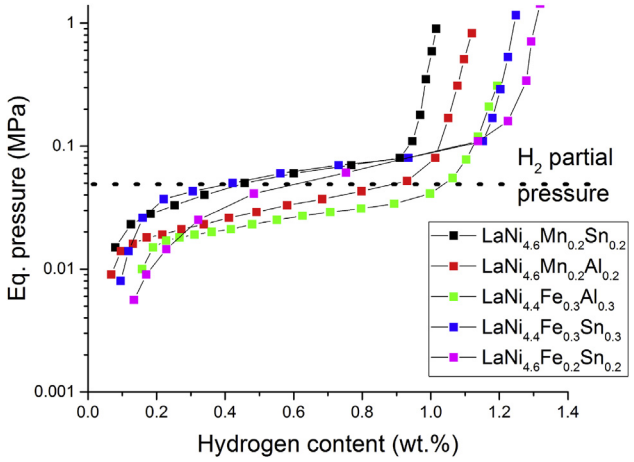

Fig. 2 – Preliminary tests. PCT isotherms of AB_5 alloys.

Alloys $LaNi_{4.4}Fe_{0.3}Al_{0.3}$ and $LaNi_{4.6}Mn_{0.2}Al_{0.2}$ samples mass of 50 g are investigated in a wide temperature range using US150 experimental setup (Figs. 3 and 4).

Absorption and desorption curves are characterized to be close enough to each other with small hysteresis. Hysteresis tends to increase slightly with increase of temperature. Coupled with small plateau slope of PCT curves, investigated alloys are good candidates for practical application in biohydrogen separation systems. Reversible capacity for both alloys does not exceed 1.1 %wt. and reduce slightly with temperature increase. Experimental data are collected and summarized in Table 1.

The alloys are supposed to be used in tubular metal hydride reactors RPS-8 [49]. Tap water (cold/hot) is used as heat exchange fluid for hydrogen sorption/desorption process. Usually cold tap water temperature is in a range 277–293 K and hot tap water temperature is 333–348 K. Thus, lower temperatures of heat exchange fluid at absorption stage can enhance hydrogen sorption kinetics and avoid heat transfer crisis [60]. Another advantage of investigated alloys is desorption pressure at higher temperatures, which is suitable for direct supply of PEM fuel cells. As usual, required pressure for PEM fuel cell supply is 0.12–0.15 MPa. Thus, almost all amount of absorbed hydrogen is available to use in fuel cell stack using low potential heat sources.

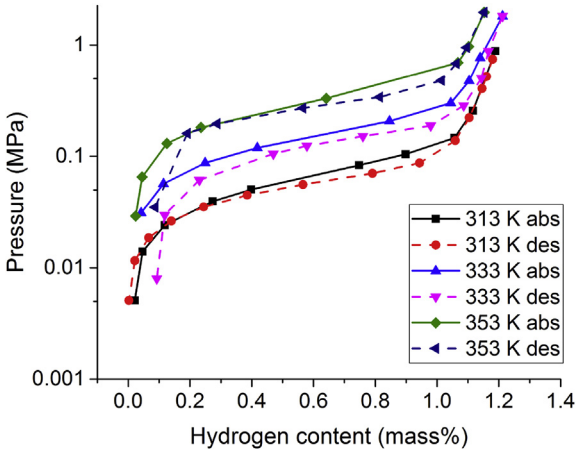

Fig. 3 – PCT diagram for $LaNi_{4.4}Fe_{0.3}Al_{0.3}$.

Metal hydride powder bed properties

Designing a practical metal-hydride storage system with respect to the different aspects of thermodynamics, kinetics and mass and energy transport requires credible modelling that is in a good agreement with the conditions experienced. Mathematical modelling is a useful tool to identify and predict the state of the metal-hydride during absorption and desorption as well as to determine the relationship between different effective factors with the aim of finding the best performance of the MH storage system [61].

Intermetallic compounds in hydrogen storage systems are activated fine powders. When hydrogen moves through such a porous bed, significant pressure drops can occur in the metal hydride storage reactor. The hydrogen pressure drop due to the hydraulic resistance of the porous bed can significantly effect on the dynamics of hydrogen sorption and desorption in the systems, where a significant amount of hydrogen is absorbed (desorbed) in a short time or the difference between inlet pressure and equilibrium pressure is small. Latter case can be occurred in biohydrogen purification systems.

The permeability of the metal hydride media is an important value characterizing the hydraulic resistance of the finely disperse powder beds. These characteristic is especially important for flow through regime used to biohydrogen separation [49]. The permeability is often determined by geometric characteristics of porous medium and does not depend on fluid properties. For metal hydride beds, it is usually calculated on the basis of the Kozeny–Carman equation, yet it is obtained for a laminar flow in the medium consisting of spherical particles with a rather thin distribution over the sizes:

$$k = \frac{1}{C}\frac{\varepsilon^3 d_p^2}{(1-\varepsilon)^2} \quad (1)$$

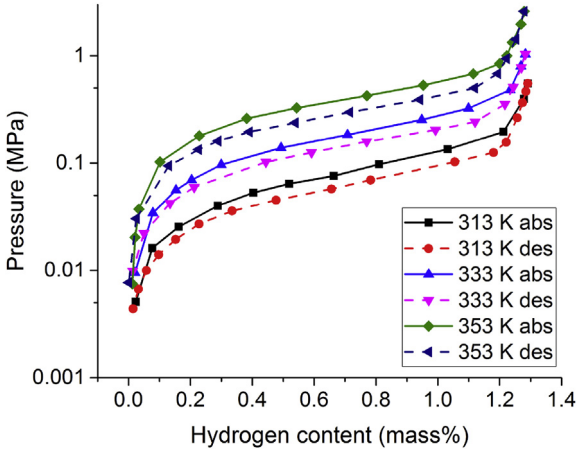

Fig. 4 – PCT diagram for $LaNi_{4.6}Mn_{0.2}Al_{0.2}$.

Table 1 – Hydrogen storage properties of AB_5 alloys.

Alloy composition	T, K	P_{abs}, MPa	P_{des}, MPa	C_{rev}, wt%	$\Delta H_{abs/des}$, kJ/mol	$\Delta S_{abs/des}$, kJ/mol K	Hysteresis ln (P_{abs}/P_{des})
$LaNi_{4.4}Fe_{0.3}Al_{0.3}$	283	0.015[a]	0.013[a]	1.1	- 36.6/36.1	113.4/110.4	0.14
	293	0.028[a]	0.024[a]				0.15
	313	0.067	0.056				0.18
	333	0.149	0.124				0.18
	353	0.33	0.27				0.2
$LaNi_{4.6}Mn_{0.2}Al_{0.2}$	283	0.016[a]	0.014[a]	1.1	- 36.6/35.0	114.4/107.2	0.13
	293	0.027[a]	0.023[a]				0.16
	313	0.076	0.058				0.27
	333	0.165	0.125				0.28
	353	0.375	0.267				0.34

[a] Values are calculated from Van't Hoff equation.

where ε is the porosity of powder bed, d_p is the average particle size, and C is a constant.

The porosity is defined as:

$$\varepsilon = 1 - \frac{\rho_e}{\rho_s} \quad (2)$$

where ρ_s is the density of the solid and ρ_e is the effective density of the powder, which depends on the degree of compression [61]. The porosity of AB_5 type alloys is typically taken to be 0.5 [62,63]. The porosity for HWT5800 is taken equal to 0.585 for numerical analysis of heat and mass transfer in metal hydride tank [64]. Experimental investigations [65] report porosity values in the range from 0.61 to 0.67. Porosities measured for vertical metal hydride tubular reactor varies along the height of powder bed from 0.54 at the bottom to 0.61 at the top affected by granular segmentation, densification and growth of agglomerates inside the bed [66,67].

Constant C can vary in wide range from 85 to 250 depending on particle nonsphericity and particle size distribution. For hypothetical spherical particles, C equals to 180. Kozeny-Carman equation is widely accepted and used extensively; it has many limitations from its inception. Moreover, this equation is a semi-empirical relation and the Kozeny-Carman constant is an empirical constant, which was proved to be not a constant and may be related to porosity. In simulation studies of metal hydride hydrogen storage systems, the permeability coefficient is usually calculated using Eq. (1) at C = 150 [62,63,68,69] or at C = 180 [70]. As well, there are many investigations, where permeability coefficient is taken as constant 1.2×10^{-11} m^2 [71], 8×10^{-12} m^2 [72], 10^{-8} m^2 [73,74].

Activated powders $LaNi_{4.4}Fe_{0.3}Al_{0.3}$ and $LaNi_{4.6}Mn_{0.2}Al_{0.2}$ after PCT measurements are analyzed by scanning electron microscopy Fig. 4. Granulometric studies showed similar particle size distribution for both alloys. Over 80% of particles are in the range 10–30 μm in both cases Fig. 5. Harmonic mean diameters are 12.27 and 11.21 μm for $LaNi_{4.4}Fe_{0.3}Al_{0.3}$ and $LaNi_{4.6}Mn_{0.2}Al_{0.2}$ alloys, respectively.

Effective powder density and specific surface area of metal hydrides are calculated from Quantochrome Nova 1200 adsorption data. Porosities of metal hydride powder beds are calculated by Eq. (2). In addition, bed permeability coefficients are calculated by Eq. (1). All the results are listed in Table 2.

Bed permeabilities of both metal hydride powders are in the same range 6.86×10^{-13} m^2 and 9.08×10^{-13} m^2 for $LaNi_{4.6}Mn_{0.2}Al_{0.2}$ and $LaNi_{4.4}Fe_{0.3}Al_{0.3}$, respectively. These values are close to that we measured and calculated based on Darcy's law earlier in tubular metal hydride reactor for hydrogen purification and storage RPS-8 [75]. Porosity and average particle size are setted as 0.56 and 10 μm for 1 kg of $LaNi_{4.8}Mn_{0.3}Fe_{0.1}$ alloy, respectively. Experimentally calculated bed permeability is equal to 4.2×10^{-13} m^2. However, Kozeny-Carman constant defined from experimental data was much lower and in the range 48–92. The bed permeability

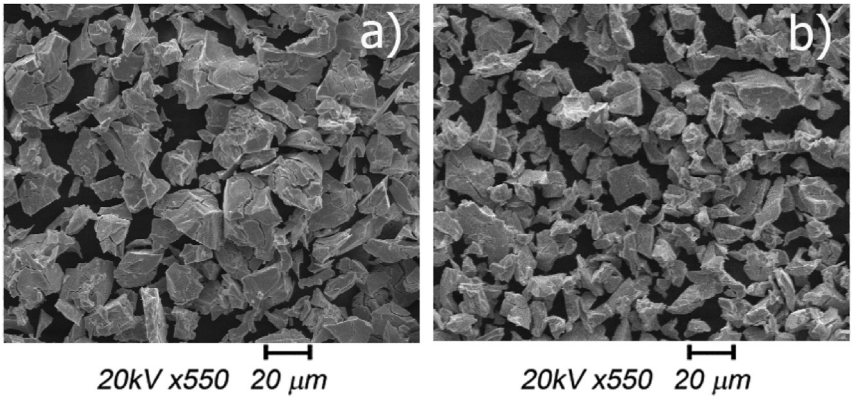

Fig. 5 – Activated powders of metal hydrides: a) $LaNi_{4.4}Fe_{0.3}Al_{0.3}$; b) $LaNi_{4.6}Mn_{0.2}Al_{0.2}$.

Table 2 – Metal hydride powder bed properties.

Alloy	$LaNi_{4.6}Mn_{0.2}Al_{0.2}$	$LaNi_{4.4}Fe_{0.3}Al_{0.3}$
Effective powder density ρ_e, g/cm^3	3.374	3.7252
Solid density ρ_s, g/cm^3	7.9947	7.937
Porosity ε	0.578	0.531
Specific surface area S, m^2/g	2.61	2.57
Mean particle size d_p, 10^{-6} m	11.2	12.3
Bed permeability at C = 150 K_{150}, 10^{-13} m^2	6.86	9.08

values taken for mathematical modelling in Refs. [76,77] are also close to ours, but it is uncertain how authors calculated them. In addition, we should note that Eq. (1) is obtained for spherical particles and this condition is not met for metal hydride particles. Applying Kozeny-Carman equation for bed permeability calculation should be done with caution and with experimentally measured porosity and particle size values.

Conclusions

Metal hydride hydrogen storage system with appropriately selected alloy composition can be a promising hydrogen separation and storage system for small-scale power plants utilizing biohydrogen as a fuel. We experimentally investigated several Ni-substituted $LaNi_5$ based alloys to meet requirements for hydrogen extraction from dilute gas streams such as biohydrogen. $LaNi_{4.4}Fe_{0.3}Al_{0.3}$ and $LaNi_{4.6}Mn_{0.2}Al_{0.2}$ are perspective materials for further pilot-scale investigations metal hydride purification reactors. Both alloys show good characteristics (low equilibrium pressures, small slope and hysteresis) for use in biohydrogen separation system.

Although, bed permeability of activated metal hydride powders is calculated from experimental data of porosity and mean particle size. Calculated values are in the same range with those measured earlier and some available in literature. Correct calculation of metal hydride bed permeability strongly depends on proper determination of porosity and mean particle size of powders.

Acknowledgement

This work is supported by the Russian Science Foundation, grant 17-19-01738. Authors would like to thank members of Laboratory for Hydrogen Energy Technologies of JIHT RAS and members of Laboratory of Energocapacious and Catalytically Active Substances of Moscow State University for discussion, useful advices and practical help in the research.

REFERENCES

[1] Dincer I, Acar C. A review on clean energy solutions for better sustainability. Int J Energy Res 2015;39(5):585–606.
[2] Zhang F, et al. The survey of key technologies in hydrogen energy storage. Int J Hydrogen Energy 2016;41(33):14535–52.
[3] International Energy Agency. World energy outlook. OECD/IEA; 2012.
[4] Hawkes FR, et al. Continuous dark fermentative hydrogen production by mesophilic microflora: principles and progress. Int J Hydrogen Energy 2007;32(2):172–84.
[5] Rahman SNA, et al. Overview biohydrogen technologies and application in fuel cell technology. Renew Sustain Energy Rev 2016;66:137–62.
[6] Claassen PAM, et al. Non-thermal production of pure hydrogen from biomass: HYVOLUTION. J Clean Prod 2010;18:S4–8.
[7] Lee D-H. Cost-benefit analysis, LCOE and evaluation of financial feasibility of full commercialization of biohydrogen. Int J Hydrogen Energy 2016;41(7):4347–57.
[8] Zech K, et al. Technical, economic and environmental assessment of technologies for the production of biohydrogen and its distribution: results of the Hy-NOW study. Int J Hydrogen Energy 2015;40(15):5487–95.
[9] Levin DB, Pitt L, Love M. Biohydrogen production: prospects and limitations to practical application. Int J Hydrogen Energy 2004;29(2):173–85.
[10] Kazakov AN, Dunikov DO, Mitrokhin SV. AB5-type intermetallic compounds for biohydrogen purification and storage. Int J Hydrogen Energy 2016;41(46):21774–9.
[11] Freeman B, Yampolskii Y. Membrane gas separation. John Wiley & Sons; 2011.
[12] Zhu X, et al. Elevated temperature pressure swing adsorption process for reactive separation of CO/CO2 in H2-rich gas. Int J Hydrogen Energy 2018;43(29):13305–17.
[13] Delgado JA, et al. Comparison and evaluation of agglomerated MOFs in biohydrogen purification by means of pressure swing adsorption (PSA). Chem Eng J 2017;326:117–29.
[14] Ohs B, Falkenberg M, Wessling M. Optimizing hybrid membrane-pressure swing adsorption processes for biogenic hydrogen recovery. Chem Eng J 2019;364:452–61.
[15] Mohamad IN, et al. Permeation properties of polymeric membranes for biohydrogen purification. Int J Hydrogen Energy 2016;41(7):4474–88.
[16] Bernardo P, Jansen JC. 14 - polymeric membranes for the purification of hydrogen. In: Subramani V, Basile A, Veziroğlu TN, editors. Compendium of hydrogen energy. Oxford: Woodhead Publishing; 2015. p. 419–43.
[17] Bakonyi P, Nemestóthy N, Bélafi-Bakó K. Biohydrogen purification by membranes: an overview on the operational conditions affecting the performance of non-porous, polymeric and ionic liquid based gas separation membranes. Int J Hydrogen Energy 2013;38(23):9673–87.
[18] Koroglu EO, et al. An integrated system development including PEM fuel cell/biogas purification during acidogenic biohydrogen production from dairy wastewater. Int J Hydrogen Energy 2019;44(32):17297–303.
[19] Bakonyi P, et al. A review of the innovative gas separation membrane bioreactor with mechanisms for integrated production and purification of biohydrogen. Bioresour Technol 2018;270:643–55.
[20] Bakonyi P, et al. Simultaneous biohydrogen production and purification in a double-membrane bioreactor system. Int J Hydrogen Energy 2015;40(4):1690–7.
[21] Wu S-Y, et al. A novel bio-cellulose membrane and modified adsorption approach in CO2/H2 separation technique for PEM fuel cell applications. Int J Hydrogen Energy 2017;42(45):27630–40.
[22] Lototskyy MV, et al. The use of metal hydrides in fuel cell applications. Prog Nat Sci: Mater Int 2017;27(1):3–20.

[23] Srinivasan SS, Demirocak DE. Metal hydrides used for hydrogen storage. In: Chen Y-P, Bashir S, Liu JL, editors. Nanostructured materials for next-generation energy storage and conversion: hydrogen production, storage, and utilization. Berlin, Heidelberg: Springer Berlin Heidelberg; 2017. p. 225–55.
[24] Zheng J, et al. Development of high pressure gaseous hydrogen storage technologies. Int J Hydrogen Energy 2012;37(1):1048–57.
[25] Wang H, Prasad AK, Advani SG. Hydrogen storage systems based on hydride materials with enhanced thermal conductivity. Int J Hydrogen Energy 2012;37(1):290–8.
[26] Lototskyy M, et al. Metal hydride hydrogen storage tank for fuel cell utility vehicles. Int J Hydrogen Energy 2019. https://doi.org/10.1016/j.ijhydene.2019.04.124.
[27] Khayrullina A, Blinov D, Borzenko V. Air heated metal hydride energy storage system design and experiments for microgrid applications. Int J Hydrogen Energy 2019;44(35):19168–76.
[28] Kubo K, Kawaharazaki Y, Itoh H. Development of large MH tank system for renewable energy storage. Int J Hydrogen Energy 2017;42(35):22475–9.
[29] Rusman NAA, Dahari M. A review on the current progress of metal hydrides material for solid-state hydrogen storage applications. Int J Hydrogen Energy 2016;41(28):12108–26.
[30] Dunikov DO, Blinov DV. Pressure artifacts at isothermal operation of a metal hydride tank. Int J Hydrogen Energy 2019;44(14):7422–7.
[31] Lototskyy MV, et al. Metal hydride hydrogen compressors: a review. Int J Hydrogen Energy 2014;39(11):5818–51.
[32] Lototskyy M, et al. Thermally driven metal hydride hydrogen compressor for medium-scale Applications. Energy Procedia 2012;29:347–56.
[33] Tarasov BP, et al. Cycling stability of RNi5 (R = La, La+Ce) hydrides during the operation of metal hydride hydrogen compressor. Int J Hydrogen Energy 2018;43(9):4415–27.
[34] Yartys VA, et al. Metal hydride hydrogen compression: recent advances and future prospects. Appl Phys A 2016;122(4):415.
[35] Guo X, et al. Laves phase hydrogen storage alloys for super-high-pressure metal hydride hydrogen compressors. Rare Met 2011;30(3):227–31.
[36] Manickam K, et al. Future perspectives of thermal energy storage with metal hydrides. Int J Hydrogen Energy 2019;44(15):7738–45.
[37] Sharma VK, Kumar EA. Studies on La based intermetallic hydrides to determine their suitability in metal hydride based cooling systems. Intermetallics 2015;57:60–7.
[38] Satheesh A, Muthukumar P. Performance investigations of a single-stage metal hydride heat pump. Int J Hydrogen Energy 2010;35(13):6950–8.
[39] Muthukumar P, Groll M. Metal hydride based heating and cooling systems: a review. Int J Hydrogen Energy 2010;35(8):3817–31.
[40] Sandrock G, Bowman RC. Gas-based hydride applications: recent progress and future needs. J Alloy Comp 2003;356–357:794–9.
[41] Sandrock G. A panoramic overview of hydrogen storage alloys from a gas reaction point of view. J Alloy Comp 1999;293–295:877–88.
[42] Sheridan Iii JJ, et al. Hydrogen separation from mixed gas streams using reversible metal hydrides. J Less Common Met 1983;89(2):447–55.
[43] Sheridan JJ, Eisenberg FG, Sandrock GD, Huston EL, Snape E, Stickles P, Cheng GC. Recovering hydrogen from gas stream using metal hydride. Patent US; 1982, 4360505.
[44] Au M, et al. The recovery, purification, storage and transport of hydrogen separated from industrial purge gas by means of mobile hydride containers. Int J Hydrogen Energy 1996;21(1):33–7.
[45] Dimanta I, et al. Metal hydride alloys for storing hydrogen produced by anaerobic bacterial fermentation. Int J Hydrogen Energy 2016;41(22):9394–401.
[46] Miura S, et al. A hydrogen purification and storage system using CO adsorbent and metal hydride. J Alloy Comp 2013;580(1):S414–7.
[47] Miura S, Fujisawa A, Ishida M. A hydrogen purification and storage system using metal hydride. Int J Hydrogen Energy 2012;37(3):2794–9.
[48] Miura, S., A hydrogen purification and storage system using metal hydride for DSS operations. 19th world hydrogen energy conference 2012, 2012.
[49] Dunikov D, et al. Biohydrogen purification using metal hydride technologies. Int J Hydrogen Energy 2016;41(46):21787–94.
[50] Lototskyy M, et al. Application of surface-modified metal hydrides for hydrogen separation from gas mixtures containing carbon dioxide and monoxide. J Alloy Comp 2013;580:S382–5.
[51] Lototsky MV, et al. Surface-modified advanced hydrogen storage alloys for hydrogen separation and purification. J Alloy Comp 2011;509(2):S555–61.
[52] Sun YM, Suda S. Studies on the fluorination method for improving surface properties and characteristics of AB5-types of hydrides. J Alloy Comp 2002;330(332):627–31.
[53] Wang XL, Iwata K, Suda S. Hydrogen purification using fluorinated LaNi4.7Al0.3 alloy. J Alloy Comp 1995;231(1–2):860–4.
[54] Liu C-M, et al. Biohydrogen production from rice straw hydrolyzate in a continuously external circulating bioreactor. Int J Hydrogen Energy 2014;39(33):19317–22.
[55] Liu C-M, et al. Biohydrogen production evaluation from rice straw hydrolysate by concentrated acid pre-treatment in both batch and continuous systems. Int J Hydrogen Energy 2013;38(35):15823–9.
[56] Malyshenko SP, Mitrokhin SV, Romanov IA. Effects of scaling in metal hydride materials for hydrogen storage and compression. J Alloy Comp 2015;645(1):S84–8.
[57] Takaguchi Y, Tanaka K. Hydriding–dehydriding characteristics of NdNi5 and effects of Sn-substitution. J Alloy Comp 2000;297(1–2):73–80.
[58] Borzone EM, et al. Stability of LaNi5–xSnx cycled in hydrogen. Int J Hydrogen Energy 2014;39(16):8791–6.
[59] Joubert JM, et al. Crystallographic study of LaNi5–xSnx ($0.2 \leq x \leq 0.5$) compounds and their hydrides. J Alloy Comp 1999;293(295):124–9.
[60] Borzenko V, Dunikov D, Malyshenko S. Crisis phenomena in metal hydride hydrogen storage facilities. High Temp 2011;49(2):249–56.
[61] Mohammadshahi SS, Gray EM, Webb CJ. A review of mathematical modelling of metal-hydride systems for hydrogen storage applications. Int J Hydrogen Energy 2016;41(5):3470–84.
[62] Kumar Phate A, Prakash Maiya M, Murthy SS. Simulation of transient heat and mass transfer during hydrogen sorption in cylindrical metal hydride beds. Int J Hydrogen Energy 2007;32(12):1969–81.
[63] Freni A, Cipitì F, Cacciola G. Finite element-based simulation of a metal hydride-based hydrogen storage tank. Int J Hydrogen Energy 2009;34(20):8574–82.
[64] Ye J, et al. Numerical analysis of heat and mass transfer during absorption of hydrogen in metal hydride based hydrogen storage tanks. Int J Hydrogen Energy 2010;35(15):8216–24.

[65] Matsushita M, Monde M, Mitsutake Y. Experimental formula for estimating porosity in a metal hydride packed bed. Int J Hydrogen Energy 2013;38(17):7056–64.
[66] Kazakov AN, et al. Experimental investigations of adsorption characteristics and porosity of activated metal hydride powders. J Phys Conf Ser 2017;891:012115.
[67] Borzenko VI, et al. Hydrogen sorption properties of metal hydride beds: effect of internal stresses caused by reactor geometry. Int J Hydrogen Energy 2019;44(12):6086–92.
[68] Chabane D, et al. Influence of the key parameters on the dynamic behavior of the hydrogen absorption by LaNi5. Int J Hydrogen Energy 2017;42(2):1412–9.
[69] Wang Y, et al. Three-dimensional modeling of hydrogen sorption in metal hydride hydrogen storage beds. J Power Sources 2009;194(2):997–1006.
[70] Nakagawa T, et al. Numerical analysis of heat and mass transfer characteristics in the metal hydride bed. Int J Hydrogen Energy 2000;25(4):339–50.
[71] Botzung M, et al. Simulation and experimental validation of a hydrogen storage tank with metal hydrides. Int J Hydrogen Energy 2008;33(1):98–104.
[72] Brown TM, et al. Accurate simplified dynamic model of a metal hydride tank. Int J Hydrogen Energy 2008;33(20):5596–605.
[73] Nam J, Ko J, Ju H. Three-dimensional modeling and simulation of hydrogen absorption in metal hydride hydrogen storage vessels. Appl Energy 2012;89(1):164–75.
[74] Chung CA, Ho C-J. Thermal–fluid behavior of the hydriding and dehydriding processes in a metal hydride hydrogen storage canister. Int J Hydrogen Energy 2009;34(10):4351–64.
[75] Blinov DV, Dunikov DO, Kazakov AN. Measuring the gas permeability of a metal hydride bed of the LaNi5 type alloy. High Temp 2016;54(1):153–6.
[76] Yang FS, Zhang ZX, Bao ZW. An extensive parametric analysis on the performance of a single-stage metal hydride heat transformer. Int J Hydrogen Energy 2012;37(3):2623–34.
[77] Yang F, et al. Identifying heat and mass transfer characteristics of metal hydride reactor during adsorption—parameter analysis and numerical study. Int J Hydrogen Energy 2008;33(3):1014–22.